

# MARRS: Masked Autoregressive Unit-based Reaction Synthesis

Yabiao Wang<sup>1,2\*</sup>, Shuo Wang<sup>2\*</sup>, Jiangning Zhang<sup>2</sup>, Jiafu Wu<sup>2</sup>, Qingdong He<sup>2</sup>, Yong Liu<sup>1†</sup>

<sup>1</sup>Zhejiang University, <sup>2</sup>Youtu Lab, Tencent

## Abstract

This work aims at a challenging task: human action-reaction synthesis, *i.e.*, generating human reactions conditioned on the action sequence of another person. Currently, autoregressive modeling approaches with vector quantization (VQ) have achieved remarkable performance in motion generation tasks. However, VQ has inherent disadvantages, including quantization information loss, low codebook utilization, *etc.* In addition, while dividing the body into separate units can be beneficial, the computational complexity needs to be considered. Also, the importance of mutual perception among units is often neglected. In this work, we propose MARRS, a novel framework designed to generate coordinated and fine-grained reaction motions using continuous representations. Initially, we present the Unit-distinguished Motion Variational AutoEncoder (UD-VAE), which segments the entire body into distinct body and hand units, encoding each independently. Subsequently, we propose Action-Conditioned Fusion (ACF), which involves randomly masking a subset of reactive tokens and extracting specific information about the body and hands from the active tokens. Furthermore, we introduce Adaptive Unit Modulation (AUM) to facilitate interaction between body and hand units by using the information from one unit to adaptively modulate the other. Finally, for the diffusion model, we employ a compact MLP as a noise predictor for each distinct body unit and incorporate the diffusion loss to model the probability distribution of each token. Both quantitative and qualitative results demonstrate that our method achieves superior performance. The code will be released upon acceptance.

## Introduction

In the field of generative computer vision, human-human motion generation holds substantial importance for computer animation (Parent 2012; Magnenat-Thalmann et al. 1985), game development (Urbain 2010; Bethke 2003), and robotic control (Saridis 1983; Wang et al. 2023a; Chen et al. 2023b; Wang et al. 2024a). Existing works primarily treat the actors and reactors equally, often neglecting the challenge of reaction generation in ubiquitous human-human interactions. In this work, we focus on generative models for human action-reaction synthesis, *i.e.*, generating human reactions based on the action sequence of another individual

as conditions, which can significantly reduce the workload for animators by enabling them to design an acting character and automatically generate meaningful motions for a reacting character.

Although autoregressive modeling approaches have recently achieved remarkable performance in motion generation tasks (Pinyoanuntapong et al. 2024), it is sub-optimal to apply these methods to human action-reaction synthesis. For example, as shown in Tab. 5 (VQ-VAE and UD-VQ-VAE), the reconstruction and generation performance is unsatisfactory. There are two challenges for this: first, vector quantization (VQ) exhibits inherent limitations. Mapping continuous motion data to a constrained set of discrete tokens inevitably results in a loss of information. Although Mo-mask (Guo et al. 2024) utilizes successive stages of residual quantization to minimize quantization errors incrementally, complex multistage training does not fundamentally eliminate quantization errors. Second, the notorious codebook collapse (Zheng and Vedaldi 2023) makes optimizing the code vectors in the existing VQ-VAE not entirely trivial. Without relying on VQ-VAE, some methods (Shi et al. 2024) have tried autoregressive diffusion in motion generation, but their cumbersome training and inference processes do not achieve stunning performance in single-segment motion generation. Moreover, units splitting has been shown to be an effective strategy in motion generation. However, as the number of units increases, the computational effort of the model also increases. And the importance of mutual perception among units is often neglected. Thus, it is necessary to explore a more rational units splitting as well as to design an efficient and effective units perception method.

Recently, some works (Li et al. 2024) have explored autoregressive image generation without vector quantization, providing new insight into autoregressive generation methods. In this paper, we propose MARRS (Fig. 1), a novel framework that generates synchronized and fine-grained reaction movements in continuous representations. During the training phase, MARRS follows a two-stage paradigm. In the first stage, for the network to learn the concept of the body and hands, we propose Unit-distinguished Motion Variational AutoEncoder (UD-VAE), which splits the whole-body into body and hands units and then encodes them independently using a variational autoencoder. In the second stage, we propose Action-Conditioned Fusion

\*Equal contributions.

†Corresponding author.

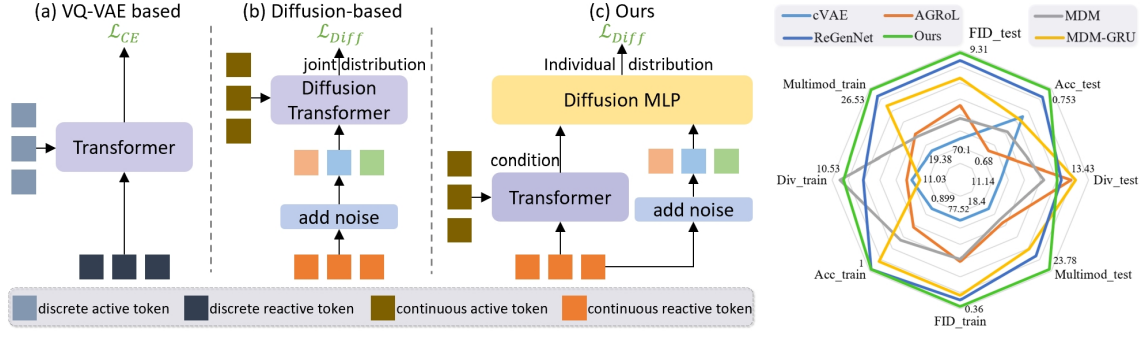


Figure 1: **Left: Paradigm comparison of different frameworks.** (a) and (b) present the structures of the VQ-VAE-based and Diffusion-based methods, respectively, while (c) shows the framework of our proposed MARRS. **Right: result comparison among our method and other methods on eight metrics.**

(ACF), which involves randomly masking out a portion of the reactive tokens and then extracting the information of body and hands from the active tokens separately using the transformer. Next, in order to avoid the lack of mutual perception between the two units (body and hands), we propose Adaptive Unit Modulation (AUM), which utilizes information from the body or hands to modulate the other unit adaptively and enables interaction between the body and hands generators to jointly produce whole-body motion. Finally, we utilize a compact MLP to serve as a noise predictor for each distinct unit, modeling individual tokens separately and integrating the diffusion loss (Li et al. 2024) to assess the probability of each token. As shown in Fig. 1, we provide a paradigm comparison of different frameworks and a result comparison among different methods.

Our contributions can be summarized as follows:

- we propose MARRS, a novel framework that generates synchronized and fine-grained reaction movements. To the best of our knowledge, this is the first successful application of masked autoregressive generation to the field of action-reaction synthesis.
- We introduce the Unit-distinguished Motion Variational AutoEncoder (UD-VAE) to enable the network to grasp the concepts of the body and hands. Next, we propose Action-Conditioned Fusion (ACF), which could extract information about the body and hands from the reactive tokens. Furthermore, to prevent the body and hands units from lacking awareness of each other, we propose Adaptive Unit Modulation (AUM). Finally, we employ a compact MLP as a noise predictor and integrate the diffusion loss to estimate the probability of each token.
- We conduct extensive experiments on the benchmark human action-reaction synthesis datasets, NTU120-AS and Chi3D-AS. The results in both online and offline settings demonstrate the effectiveness of our proposed methods.

## Related Work

### Motion Generation Framework

TEMOS (Petrovich, Black, and Varol 2022) and T2M (Guo et al. 2022) use a Transformer-based VAE combined with

a text encoder to create motion sequences from textual descriptions. T2M-GPT (Zhang et al. 2023a) introduces a framework based on VQ-VAE and Generative Pretrained Transformer (GPT) for motion generation. MMM (Pinyoanuntapong et al. 2024) proposes a conditional masked motion architecture based on VQ-VAE. To mitigate quantization errors, MoMask (Guo et al. 2024) introduces a hierarchical quantization scheme. MotionDiffuse (Zhang et al. 2024) and MDM (Tevet et al. 2022) are groundbreaking frameworks for text-driven motion generation using diffusion models. Instead of using a diffusion model to connect raw motion sequences with conditional inputs, MLD (Chen et al. 2023a) employs a latent diffusion model to significantly reduce training and inference costs. ReMoDiffuse (Zhang et al. 2023b) introduces an enhancement mechanism based on dataset retrieval to improve the denoising process in diffusion models.

### Human-Human Motion Generation

Synthesizing human-human interactions is essential for applications in gaming and augmented/virtual reality. Earlier approaches often utilized motion graphs (Shum, Komura, and Yamazaki 2007) and momentum-based inverse kinematics (Komura, Ho, and Lau 2005) to simulate the movements of human joints. Recently, more sophisticated techniques have emerged. ComMDM (Shafir et al. 2023) refines a pre-trained text-to-motion diffusion model using a limited dataset of two-person motions. RIG (Tanaka and Fujiwara 2023) transforms the text describing asymmetric interactions into both active and passive forms to ensure consistent textual context for each participant. To facilitate the interaction by positioning the joints of two individuals accurately, InterControl (Wang et al. 2023b) leverages a Large Language Model to create movement plans through carefully crafted prompts. InterGen (Liang et al. 2024) introduces a diffusion model with shared parameters and several regularization losses. Designing an efficient approach to modeling between two people, TIMotion (Wang et al. 2024b) proposes a temporal and interactive framework. FreeMotion (Fan et al. 2024) proposes to integrate the single and multi-person motion by the conditional motion distribution.

Based on the premise of actor’s motion, ReGenNet (Xu et al. 2024) proposes a diffusion-based generative model and explicit distance-based interaction loss.

### Autoregressive Modeling without Quantization

MAR (Li et al. 2024) initially utilizes autoregressive models within a continuous-valued domain to represent the probability distribution of each token through a diffusion process. MarDini (Liu et al. 2024) employs MAR for temporal planning, allowing for video generation based on any number of masked frames at various frame positions. MMAR (Yang et al. 2024) processes continuous-valued image tokens to prevent information loss and separates the diffusion process from the autoregressive model in the context of multi-modal large language models. AMDM (Shi et al. 2024) utilizes the diffusion model to implement frame-by-frame incremental generation. MARDM (Meng et al. 2024) presents a human motion diffusion model capable of executing bidirectional masked autoregression.

## Method

### Problem Formulation

In the context of synthesizing human action-reaction sequences, our objective is to produce a reaction that is conditioned on a given action. Formally, given that the reaction sequence  $x^{1:N} = \{x^i\}_{i=1}^N$  and the action sequence  $y^{1:N} = \{y^i\}_{i=1}^N$ , our goal is to model the conditional probability distribution  $P(x^{1:N}|y^{1:N})$ , enabling us to sample realistic reactive motions. As with (Xu et al. 2024), we utilize the SMPL-X (Pavlakos et al. 2019) human model to represent the sequence of human motions. Thus, the reaction can be represented as  $x^i = [\theta_i^x, q_i^x, \gamma_i^x]$ , where  $\theta_i^x \in \mathbb{R}^{3K}$ ,  $q_i^x \in \mathbb{R}^3$ ,  $\gamma_i^x \in \mathbb{R}^3$  are the pose parameters, global orientation, and root translation of the person. Here,  $K$  is set to 54 representing the number of body joints, including the jaw, eyeballs, and fingers.

### Overview of MARRS

Our method consists of two stages to generate the reactive motions on the premise that one’s actions are known. In the first stage, we split the whole-body motion into two units: body and hands, and then map them to continuous-valued tokenizers. In the second stage, the reactive token of each unit initially gathers information from the active token via Action-Conditioned Fusion. Subsequently, different units gain coordinated information through Adaptive Unit Modulation. Finally, we utilize a compact MLP as a noise predictor and incorporate the diffusion loss to model each token. The overall structure is shown in Fig. 2.

### Unit-distinguished Motion VAE (UD-VAE)

In the first stage, we split the whole-body motion into two units: body and hands. Then each unit is encoded independently by a variational autoencoder (VAE), thereby providing prior knowledge about the concept of body and hands.

Specifically, given an active motion sequence  $y^{1:N}$ , we separate it into two units  $\{y_k^{1:N}, k \in [body, hands]\}$ . Then

the unit  $y_k^{1:N}$  is fed into the corresponding  $Encoder_k$  to obtain the embedding  $E_k^{1:L}$ , where  $L = \frac{N}{r}$  and  $r$  is the down-sampling rate of the encoder. Next, the Gaussian distribution parameters  $\mu_k^{1:L}$  and  $\Sigma_k^{1:L}$  are obtained through a linear layer, and we sample latent vectors  $z \in \mathbb{R}^d$  from the above distributions. The latent dimension  $d$  is set to 256 in our experiments. Finally, the sampled vectors are input into the  $Decoder_k$  to obtain the reconstructed  $k$ -th unit  $\hat{y}_k^{1:N}$ .

Similarly, we can acquire the reconstructed  $k$ -th unit  $\hat{x}_k^{1:N}$  for the reactive motion sequence  $x^{1:N}$ . The optimization objective of the  $k$ -th unit’s VAE is:

$$\mathcal{L}_{VAE}^k = \text{SmoothL1}(\hat{x}_k^{1:N}, x_k^{1:N}) + \text{SmoothL1}(\hat{y}_k^{1:N}, y_k^{1:N}). \quad (1)$$

The structure of the UD-VAE is shown in Fig. 2. The encoder and decoder adopt 1D ResNet-based network, which is the same as T2M-GPT (Zhang et al. 2023a).

### Masked Reaction Generation Model

In the second stage, we introduce the reaction generation framework as shown in Fig. 2, which consists of Action-Conditioned Fusion, Adaptive Unit Modulation, and diffusion MLPs belonging to their respective units.

**Action-Conditioned Fusion (ACF).** During training, action and reaction are sent to UD-VAE respectively, and continuous-valued tokenizers corresponding to body and hands are obtained after the encoder. To enable the networks to be aware of the conception of different whole-body units, we use two networks with the same structure but no shared parameters for the body and hands. First, we define the computation of Attn as:

$$\text{Attn}(Q, K, V) = \text{softmax}\left(\frac{(QW^Q) \cdot (KW^K)^T}{\sqrt{C}}\right) \cdot (VW^V), \quad (2)$$

where  $W^Q$ ,  $W^K$ , and  $W^V$  are trainable weights.

Specifically, given the continuous-valued **body tokens** of actor  $Y_b$  and reactor  $X_b$ , we further extract the actor’s motion information  $Y'_b$  through Attn and obtain the refined token embeddings  $Y'_b$  as:

$$Y'_b = \text{Attn}(Y_b, Y_b, Y_b). \quad (3)$$

Next, we randomly mask out a varying fraction of sequence elements  $X_b$  by replacing the tokens with a special [MASK] token and the resulting sequence is denoted as  $\hat{X}_b$ . Our goal is to predict the masked tokens given  $\hat{X}_b$  and the active tokens  $Y'_b$ . Then the reactive token embedding  $\hat{X}_b^{fusion}$  incorporating the action information can be obtained as follows:

$$\hat{X}_b' = \text{Attn}(\hat{X}_b, \hat{X}_b, \hat{X}_b), \quad (4)$$

$$\hat{X}_b^{fusion} = \text{Attn}(\hat{X}_b', Y'_b, Y'_b). \quad (5)$$

For the continuous-valued **hands tokens** ( $Y_h, X_h$ ) of the actor and reactor, we can acquire the reactive token embedding  $\hat{X}_h^{fusion}$  in the same way as above.

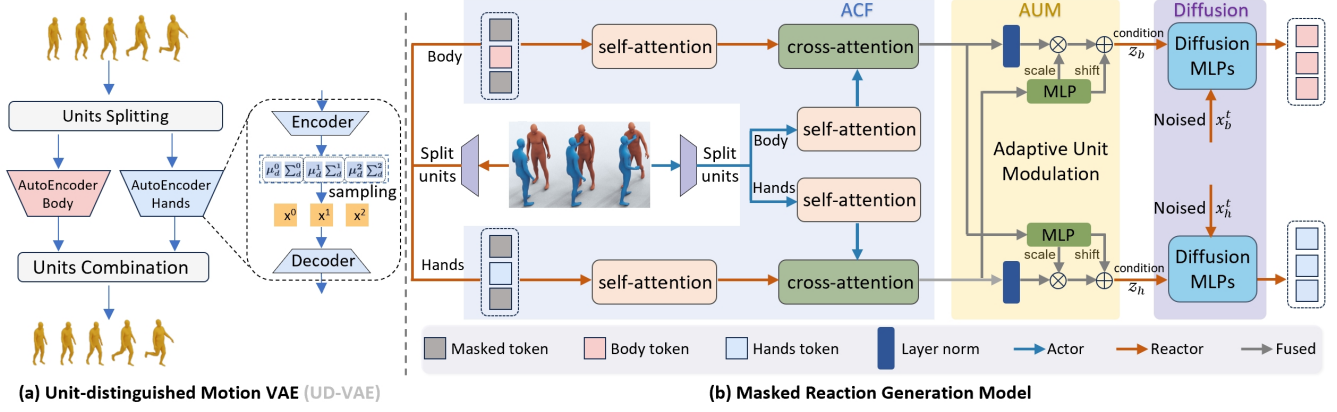


Figure 2: **The overall framework of our proposed MARRS.** (a) Whole-body motion is divided into two units: body and hands and then each unit is encoded independently by a VAE. (b) shows the process of the masked reaction generation model.

**Adaptive Unit Modulation (AUM).** The whole-body motion can be divided into two units: the body unit and the hands unit. As noted in (Zou et al. 2024), depending exclusively on these individual unit motion generators may fail to produce coordinated whole-body motions, as they lack awareness of other units. Hence, we propose AUM, which enables interaction between the body and hands generators to jointly produce whole-body motion.

Given that the reactive token embeddings  $\hat{X}_b^{fusion}$  and  $\hat{X}_h^{fusion}$  from ACF, we utilize the body’s information to adaptively modulate and optimize the position of the hands. The modulated hands embeddings  $\hat{X}_h^{final}$  are acquired as follows:

$$scale_b, shift_b = \text{Linear}(\hat{X}_b^{fusion}), \quad (6)$$

$$\hat{X}_h^{final} = scale_b \cdot \text{LN}(\hat{X}_h^{fusion}) + shift_b. \quad (7)$$

where LN denotes the layer normalization. Similarly, we can obtain the modulated body embeddings  $\hat{X}_b^{final}$  as:

$$scale_h, shift_h = \text{Linear}(\hat{X}_h^{fusion}), \quad (8)$$

$$\hat{X}_b^{final} = scale_h \cdot \text{LN}(\hat{X}_b^{fusion}) + shift_h. \quad (9)$$

**Diffusion for Autoregressive Reaction Generation.** Autoregressive methods (Pinyoanuntapong et al. 2024; Guo et al. 2024) have shown considerable benefits in motion generation. Instead of modeling the jointed distribution of all tokens, autoregressive models formulate the generation task as “next token prediction”:

$$p(x^1, \dots, x^n) = \prod_{i=1}^n p(x^i | x^1, \dots, x^{i-1}), \quad (10)$$

where  $\{x^1, x^2, \dots, x^n\}$  is the sequence of tokens and the superscript  $1 \leq i \leq n$  specifies an order.

As noted in MAR (Li et al. 2024), training diffusion models by employing MSE loss to carry out autoregressive generation leads to a disastrous FID score because of the failure of capturing chained probability distributions. Motivated by the successful application of MAR in image generation, we

incorporate the diffusion loss (Li et al. 2024) to estimate the probability of each token within the field of the reaction generation.

Given that the modulated body embedding  $\hat{X}_b \in \mathbb{R}^{L \times d}$  and hands embedding  $\hat{X}_h \in \mathbb{R}^{L \times d}$ , where  $L$  is the number of tokens. Each token we sample from  $\hat{X}_b$  and  $\hat{X}_h$  are denoted as  $z_b \in \mathbb{R}^d$  and  $z_h \in \mathbb{R}^d$ , and we define the corresponding ground truth tokens as  $x_b$  and  $x_h$ . The loss function can be formulated as a denoising criterion:

$$\mathcal{L}(x | z) = \mathbb{E}_{\epsilon_1, t} \left[ \|\epsilon_1 - \epsilon_{\theta_1}(x_b^t | t, z_b)\|^2 \right] + \mathbb{E}_{\epsilon_2, t} \left[ \|\epsilon_2 - \epsilon_{\theta_2}(x_h^t | t, z_h)\|^2 \right]. \quad (11)$$

Here  $\epsilon_1 \in \mathbb{R}^d$  and  $\epsilon_2 \in \mathbb{R}^d$  are Gaussian vectors sampled from  $\mathcal{N}(\mathbf{0}, \mathbf{I})$ . The noise-corrupted data are  $x_b^t = \sqrt{\bar{\alpha}_t}x_b + \sqrt{1 - \bar{\alpha}_t}\epsilon_1$  and  $x_h^t = \sqrt{\bar{\alpha}_t}x_h + \sqrt{1 - \bar{\alpha}_t}\epsilon_2$ , where  $\bar{\alpha}_t$  is a noise schedule (Nichol and Dhariwal 2021) indexed by a time step  $t$ . We model individual tokens by using a small MLP as a noise predictor for each unit separately. The noise estimators  $\epsilon_{\theta_1}$  and  $\epsilon_{\theta_2}$  have the same structure but do not share parameters. The notation  $\epsilon_{\theta}(x_n^t | t, z_n)$  means that this network takes  $x_n^t$  as the input, and is conditional on both  $t$  and  $z_n$ .

**Inference.** Given the active motion sequence, we send them to the encoder of UD-VAE to get active tokens. We expect to generate the entire reactive tokens in  $T$  iterations in an autoregressive manner and the mask ratio in each iteration  $t$  is determined by a decay scheduling function  $\cos(\frac{\pi t}{2T})$ . First, we mask out all the reactive tokens, and feed the active and reactive tokens to ACF and AUM. Second, we take out the tokens that need to be unmasked from the predefined permuted sequences, and send them into the diffusion as conditions. Next, the tokens after sampling are regarded as the new reactive tokens, and the other tokens are masked again until the completion of the  $T$  iterations. As for the diffusion procedure, we sample  $x_n^T$  from a random Gaussian noise  $\mathcal{N}(\mathbf{0}, \mathbf{I})$ . This initial sample is then progressively denoised in a step-by-step manner, transforming  $x_n^T$  to  $x_n^0$ .

Method	Train conditioned				Test conditioned			
	FID↓	Acc.↑	Div.→	Multimod.→	FID↓	Acc.↑	Div.→	Multimod.→
Real	0.09±0.00	1.000±0.0000	10.54±0.06	26.71±0.62	0.09±0.00	0.867±0.0002	13.06±0.09	25.03±0.23
cVAE (Kingma, Welling et al. 2013)	77.52±7.25	0.899±0.0002	10.10±0.02	19.38±0.16	70.10±3.42	0.724±0.0002	11.14±0.04	18.4±0.26
AGRoL (Du et al. 2023)	38.04±1.45	0.932±0.0001	10.95±0.07	21.44±0.34	44.94±2.46	0.680±0.0001	12.51±0.09	19.73±0.17
MDM (Tevet et al. 2022)	40.13±3.65	0.955±0.0001	<b>10.53±0.04</b>	21.15±0.26	54.54±3.94	0.704±0.0003	11.98±0.07	19.45±0.20
MDM-GRU (Tevet et al. 2022)	5.31±0.18	0.993±0.0000	11.03±0.06	25.04±0.36	24.25±1.39	0.720±0.0002	<b>13.43±0.09</b>	22.24±0.29
ReGenNet (Xu et al. 2024)	0.90±0.01	<b>1.000±0.0000</b>	10.69±0.05	26.25±0.35	11.00±0.74	0.749±0.0002	13.80±0.16	22.90±0.14
Ours	<b>0.36±0.02</b>	<b>1.000±0.0000</b>	<u>10.57±0.06</u>	<b>26.53±0.20</b>	<b>9.31±0.36</b>	<b>0.753±0.0003</b>	14.05±0.09	<b>23.78±0.31</b>

Table 1: **Comparison to state-of-the-arts** on the *online, unconstrained* setting for human action-reaction synthesis on NTU120-AS (Xu et al. 2024). ± indicates 95% confidence interval, → means that closer to Real is better. **Bold** indicates best result and underline indicates second best.

Settings	Train conditioned				Test conditioned			
	FID↓	Acc.↑	Div.→	Multimod.→	FID↓	Acc.↑	Div.→	Multimod.→
Real	0.094±0.0003	1.000±0.00	10.542±0.0632	26.709±0.6193	0.085±0.0003	0.867±0.0002	13.063±0.0908	25.032±0.2332
w.o. Unit Division	0.791±0.0107	<b>1.000±0.00</b>	10.618±0.0176	26.252±0.259	14.998±0.8024	0.745±0.0002	13.867±0.1459	23.517±0.2090
Upper & Lower (Ghosh et al. 2021)	0.718±0.2524	<b>1.000±0.00</b>	<u>10.576±0.0479</u>	26.270±0.3119	<u>10.208±0.2587</u>	0.745±0.0002	14.079±0.1943	<b>23.794±0.2376</b>
6-Unit Division (Zou et al. 2024)	<b>0.214±0.0025</b>	<b>1.000±0.00</b>	10.503±0.0378	<u>26.522±0.3148</u>	14.965±0.8164	<b>0.769±0.0001</b>	<b>13.302±0.1301</b>	23.006±0.2964
Body & Hands (Ours)	<u>0.356±0.0167</u>	<b>1.000±0.00</b>	<b>10.574±0.0620</b>	<b>26.533±0.1965</b>	<b>9.312±0.3564</b>	<u>0.753±0.0003</u>	14.053±0.0912	<u>23.781±0.3102</u>

Table 2: **Ablation studies on the Unit Division.** “w.o. Unit Division” represents keeping whole-body as a complete unit. “Upper & Lower” represents dividing whole-body into the upper-and-lower-body proposed by SCA (Ghosh et al. 2021). “6-Unit Division” represents dividing whole-body into six separate units proposed by ParCo (Zou et al. 2024). Our proposed approach achieves a more balanced performance overall under train-conditioned and test-conditioned settings.

through the iterative process defined by

$$x_n^{t-1} = \frac{1}{\sqrt{\alpha_t}} \left( x_n^t - \frac{1 - \alpha_t}{\sqrt{1 - \alpha_t}} \epsilon_\theta(x_n^t | t, z_n) \right) + \sigma_t \epsilon, \quad (12)$$

where  $\sigma_t$  represents the noise level at time step  $t$ , and  $\epsilon$  is sampled from the Gaussian distribution  $\mathcal{N}(\mathbf{0}, \mathbf{I})$ . Ultimately, the decoder in UD-VAE is used to decode all tokens and convert them back into reaction sequences. The overall inference flowchart is shown in the *supplementary materials*.

## Experiments

### Experimental Setup

**Datasets.** Following (Xu et al. 2024), we evaluate our framework on NTU120-AS and Chi3D-AS using SMPL-X (Pavlakos et al. 2019) models and actor-reactor annotations. NTU120-AS contains 8,118 interaction sequences from 26 actions, captured by 3 cameras. Following (Xu et al. 2024), we use camera 1 and the cross-subject protocol (half subjects for training, half for testing). Chi3D-AS results are in the *supplementary materials*.

**Metrics.** We employ the same evaluation metrics as (Xu et al. 2024), which are as follows: (1) *Frechet Inception Distance (FID)*: measures the latent distribution distance between the generated dataset and the real dataset. (2) *Accuracy of action recognition (Acc)*: assesses action-motion matching. (3) *Diversity (Div)*: measures motion diversity in the generated motion dataset. (4) *Multimodality (MultiMod)*: indicates diversity within the same active motion. We generate 1,000 samples 20 times with different random seeds and report the average along with the 95% confidence interval.

**Settings.** The *online* setting refers to instant human action-reaction synthesis without the ability to see future motions. Conversely, the *offline* setting alleviates the need for strict synchronicity. The *unconstrained* setting means that the actor’s intention is not visible to the reactor. In the *train-conditioned* setting, the actor motions are sampled from the training set. As for the *test-conditioned* setting, the actor motions are sampled from the testing set.

### Comparisons with State-of-the-arts

**Quantitative Results.** Following (Xu et al. 2024), we mainly focus on the challenging and practical *online, unconstrained* setting. The overall results are shown in Tab. 1. In the train-conditioned setting, our method achieves state-of-the-art performance in terms of FID, action recognition accuracy, and multi-modality on the NTU120-AS dataset. This demonstrates that our model effectively learns the reaction patterns. As for the test-conditioned setting, our method achieves the best FID, action recognition accuracy, and multi-modality, especially FID, which is much better than other VAE-based and diffusion-based methods, which verifies that our method has better generalization ability. Offline setting results are in the *supplementary materials*.

**Qualitative Comparisons.** In Fig. 3, we provide a qualitative comparison between ReGenNet (Xu et al. 2024) and our proposed MARRS. It can be seen that the human reaction synthesized by our method has more reasonable relative positions and body movements. In particular, our method can generate more natural and plausible hand gestures due to modeling body and hands effectively. We provide more qualitative results in the *supplementary materials*.

Settings	Train conditioned				Test conditioned			
	FID↓	Acc.↑	Div.→	Multimod.→	FID↓	Acc.↑	Div.→	Multimod.→
Real	0.094±0.0003	1.000±0.00	10.542±0.0632	26.709±0.6193	0.085±0.0003	0.867±0.0002	13.063±0.0908	25.032±0.2332
Concatenate Fuse (Xu et al. 2024)	0.536±0.0093	0.999±0.00	10.635±0.0562	26.472±0.1958	11.302±0.7041	0.743±0.0002	14.095±0.1040	<b>24.405±0.5096</b>
Cooperative Transformer (Liang et al. 2024)	0.589±0.2348	<b>1.000±0.00</b>	10.60±0.0470	26.291±0.3186	10.267±0.2674	0.752±0.0003	<b>13.849±0.1702</b>	23.785±0.2024
ACF (Ours)	<b>0.356±0.0167</b>	<b>1.000±0.00</b>	<b>10.574±0.0620</b>	<b>26.533±0.1965</b>	<b>9.312±0.3564</b>	<b>0.753±0.0003</b>	<b>14.053±0.0912</b>	23.781±0.3102

Table 3: **Ablation studies on Action-Conditioned Fusion (ACF)**. “Concatenate Fuse” is a method proposed by ReGenNet (Xu et al. 2024) for a reactor to get information from an actor. “Cooperative Transformer” is a transformer structure designed by InterGen (Liang et al. 2024). Our approach achieves SoTA on almost all metrics.

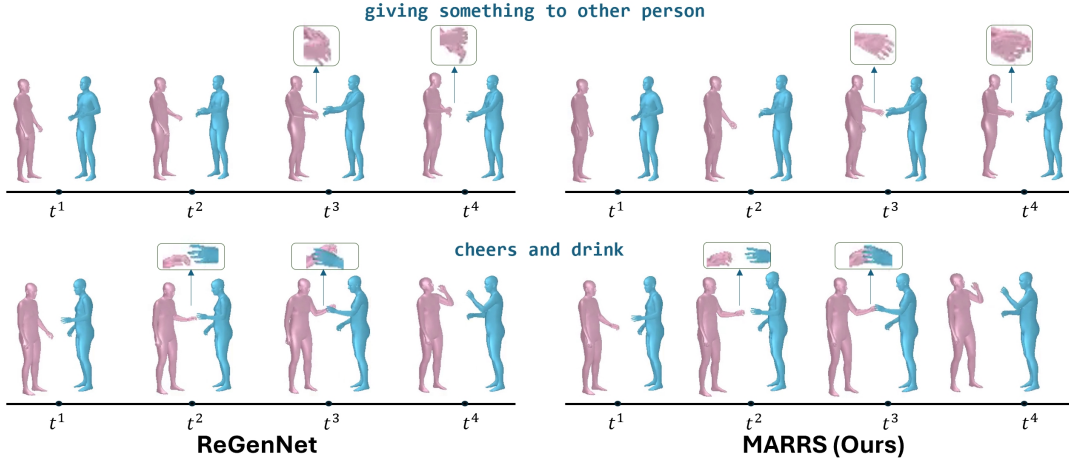


Figure 3: Qualitative comparison with ReGenNet on human reaction synthesis. Blue for actors and Red for reactors.

## Ablation Study

In this section, we carry out extensive ablation experiments to investigate the effectiveness of the crucial components in MARRS, thus offering a more profound understanding of our method. Unless specified otherwise, we conduct all the ablations on the NTU120-AS dataset under the *online, unconstrained* setting. Model scalability and complexity details are in the *supplementary materials*.

**Unit Division: Body and Hands.** In order to explore the necessity of dividing the whole-body into the body and hands units in the human reaction synthesis, we conduct the experiments on three methods: (i) keeping whole-body as a complete unit without unit division, (ii) dividing it into the upper-and-lower-body proposed by SCA (Ghosh et al. 2021), (iii) dividing it into six separate units proposed by ParCo (Zou et al. 2024). Except for three different dividing ways, the training of the first stage VAE and the structure of the second stage model are exactly the same. The results are shown in Tab. 2. There is a significant decrease in FID, Acc, and MultiMod in the test-conditioned setting without unit-division. The performance of FID and MultiMod in the test-conditioned setting increase somewhat after applying the upper-and-lower-body division. When performing the 6-unit division, FID under train-conditioned and Acc under test-conditioned achieve the best results, however, FID under test-conditioned shows almost no improvement compared to w.o. unit division, and *increasing the number of division units makes training and inference more cumbersome*.

*some and slower*. In contrast, our approach achieves more balanced results under train- and test-conditioned settings, while Div and MultiMod (train-conditioned) and FID (test-conditioned) achieve the best performance.

**Action-Conditioned Fusion (ACF).** To demonstrate the effectiveness of ACF, we additionally try two actor-reactor interactions, (i) concatenate fuse proposed by ReGenNet (Xu et al. 2024), and (ii) cooperative transformer proposed by InterGen (Liang et al. 2024). The experimental results are shown in Tab. 3. Concatenate fuse only performs well on Multimod under test-conditioned, while the performance of all other metrics is unsatisfactory. After applying cooperative transformer, FID, Acc and Div under test-conditioned are improved to some extent. Compared with others, our proposed ACF obtains optimal performance in all four metrics under train-conditioned as well as FID and Acc under test-conditioned, proving that ACF can capture the motion patterns of the two persons well.

**Adaptive Unit Modulation (AUM).** As noted in ParCo (Zou et al. 2024), communication between units is extremely important for generating stable whole-body motions. In this section, we delve into the effects of different communication ways on the model performance. We conduct the following sets of experiments: (i) no communication between different units, (ii) unit communication using the coordination layer proposed by ParCo (Zou et al. 2024), and (iii) only hands-to-body unidirectional information transfer using our proposed AUM, (iiii) only



Settings	Train conditioned				Test conditioned			
	FID↓	Acc.↑	Div.→	Multimod.→	FID↓	Acc.↑	Div.→	Multimod.→
Real	0.094±0.0003	1.000±0.00	10.542±0.0632	26.709±0.6193	0.085±0.0003	0.867±0.0002	13.063±0.0908	25.032±0.2332
w.o. Unit Communication	0.860±0.4336	<b>1.000±0.00</b>	10.630±0.0476	26.161±0.3280	13.087±0.4838	0.738±0.0002	13.904±0.1214	23.159±0.3862
Coordination Layer (Zou et al. 2024)	0.605±0.0119	<b>1.000±0.00</b>	10.616±0.0441	26.297±0.3194	10.055±0.4638	0.739±0.0002	14.178±0.1677	23.601±0.2656
AUM (Hands → Body)	0.849±0.0125	0.999±0.00	10.614±0.0535	26.216±0.1645	13.694±0.9316	0.744±0.0004	<b>13.722±0.1118</b>	22.784±0.1875
AUM (Body → Hands)	0.574±0.0120	<b>1.000±0.00</b>	10.628±0.0556	26.360±0.1893	10.533±0.6115	0.734±0.0003	14.199±0.1243	23.297±0.2799
AUM (Ours)	<b>0.356±0.0167</b>	<b>1.000±0.00</b>	<b>10.574±0.0620</b>	<b>26.533±0.1965</b>	<b>9.312±0.3564</b>	<b>0.753±0.0003</b>	14.053±0.0912	<b>23.781±0.3102</b>

Table 4: **Ablation studies on Adaptive Unit Modulation (AUM)**. “w.o. Unit Communication” indicates that the body and hands branches do not interact with each other. “Coordination Layer” is a method proposed by ParCo (Zou et al. 2024) for transferring information between different units. “Hands → Body” and “Body → Hands” represent a unidirectional transfer of information between units. Our approach achieves SoTA on almost all metrics.

body-to-hands unidirectional information transfer using our proposed AUM. The experimental results are shown in Tab. 4. Without communication, metrics under train- and test-conditioned settings worsen but without catastrophic decline (Zou et al. 2024) seen in text-to-motion. And FID under both train-conditioned and test-conditioned was significantly improved after the use of the coordination layer, proving that the exchange of information between different units is still essential in human reaction synthesis. Next, we tried two unidirectional information transfer utilizing our proposed AUM. Using AUM unidirectionally, hands-to-body transfer degrades some metrics, while body-to-hands transfer improves overall performance. This demonstrates that using only the local information of the hands does not provide the body with sufficiently accurate positional information, and that, instead, it is feasible to leverage the body’s information to optimize the details of the hands. Ultimately, the bidirectional communication of AUM achieves the best performance for all metrics under train-conditioned and FID, Acc, and Multimod under test-conditioned, demonstrating the effectiveness of our proposed AUM and the necessity of bidirectional unit communication.

Method	Reconstruction		Generation	
	FID↓	Acc.↑	FID↓	Acc.↑
VQ-VAE (AR)	10.06±0.32	0.783±0.0002	—	—
UD-VQ-VAE (AR)	5.76±0.26	0.805±0.0002	53.57±6.35	0.562±0.0004
ACTOR (VAE)	1.21±0.23	0.823±0.0002	20.16±0.65	0.730±0.0004
AMDM (AR Diffusion)	—	—	23.46±1.39	0.718±0.0002
L2 Loss (VAE)	0.18±0.10	0.866±0.0001	15.95±1.93	0.760±0.0002
MARRS (Ours)	0.18±0.10	0.866±0.0001	9.31±0.36	0.753±0.0003

Table 5: **Ablation studies on different framework**. “VQ-VAE” is based on MMM (Pinyoanuntapong et al. 2024). “UD-VQ-VAE” is based on “VQ-VAE” by applying our proposed unit division (UD). “ACTOR” (Petrovich, Black, and Varol 2021) is a VAE-based generation method. “AMDM” (Shi et al. 2024) is an autoregressive (AR) diffusion method. “L2 Loss” means directly using L2 Loss instead of incorporating diffusion loss.

**Diffusion for Autoregressive (AR) Reaction Generation.** Since AR generation is often accompanied by vector quantization (VQ), we first investigate the performance of VQ-based methods in human reaction synthesis. As shown

in Tab. 5, VQ-VAE (AR) performs poorly (10.06 FID) in the first reconstruction phase, and the failed reconstruction means that the second generation phase is not feasible. Meanwhile, we apply the unit-division way in our proposed Unit Division to VQ-VAE and name it UD-VQ-VAE (AR). The results of the reconstruction are significantly improved, but it still performs poorly in the generation phase (53.57 FID). What is more, we apply ACTOR (VAE) (Petrovich, Black, and Varol 2021) and AMDM (AR Diffusion) (Shi et al. 2024) to human reaction, but neither FID nor accuracy achieves satisfactory performance. In addition, we explore not incorporating the diffusion loss in the second stage, but directly using L2 Loss to learn the corresponding continuous motion tokens, which resulted in a drastic deterioration of FID, proving that the diffusion loss is necessary.

## Accuracy of Hand Poses and Global Translation

We used coordinate-based metrics (*APE* and *AVE*) to measure the accuracy of hand poses and global translation (root) with SOTA. As shown in Tab. 6, our method is more accurate in hand modeling, demonstrating the effectiveness of unit division and interaction. The error of global translation is also significantly smaller than that of ReGenNet, further highlighting the effectiveness of the MARRS framework.

Methods	APE (Hands)↓	AVE (Hands) ↓	APE (Root)↓	AVE (Root) ↓
ReGenNet	0.420±.0001	0.446±.0355	0.327±.0001	0.055±.0011
MARRS(Ours)	<b>0.388±.0001</b>	<b>0.430±.0357</b>	<b>0.294±.0001</b>	<b>0.043±.0010</b>

Table 6: **Comparison on hands and global translation.**

## Conclusion

In this paper, we introduce an innovative framework named MARRS, designed to generate synchronized and fine reactions. Initially, we present the UD-VAE, which divides the whole body into distinct units: body and hands, allowing for independent encoding. Following this, we introduce ACF, a process that involves randomly masking reactive tokens and then extracting information of the body and hands from the remaining active tokens. To enable whole-body collaboration, we propose AUM, which uses information from either the body or hands to adaptively adjust the other unit. Finally, in our diffusion model, we utilize a compact MLP

as a noise predictor for each specific unit and integrate diffusion loss to capture the probability distribution of each token. Both quantitative and qualitative evaluations indicate that our method outperforms existing methods.

## Supplementary Material

### Implementation Details

For the first stage, the tokenizer consists of a 3-layer encoder-decoder architecture, featuring a hidden dimension of 256, and the batch size is set to 256. For the reaction generation, the transformer consists of 8 layers with a latent dimension of 384, and the diffusion MLPs are composed of 3 layers, each with a hidden dimension of 1024. The AdamW optimizer (Loshchilov and Hutter 2017) is utilized with  $\beta_1 = 0.5$  and  $\beta_2 = 0.99$  and the batch size for this configuration is set to 128. For the training of all models, the learning rate attains  $2e-4$  following 1000 iterations, utilizing a linear warm-up schedule.

### Inference Process

Given the active motion sequence, we send it to the encoder of UD-VAE to get active tokens. We expect to generate the entire reactive tokens in  $T$  iterations in an autoregressive manner, and the mask ratio in each iteration  $t$  is determined by a decay scheduling function  $\cos(\frac{\pi t}{2T})$ . First, all reactive tokens are masked. Active and reactive tokens are fed to ACF and AUM. Second, we take out the tokens that need to be unmasked from the predefined permuted sequences and send them into the compact diffusion (very small, 3-layer MLP) as conditions. Next, the tokens after sampling are regarded as the new reactive tokens, and the other tokens are masked again until the completion of the  $T$  iterations. As for the diffusion procedure, we sample  $x_n^T$  from a random Gaussian noise  $\mathcal{N}(\mathbf{0}, \mathbf{I})$ . This initial sample is then progressively denoised in a step-by-step manner, transforming  $x_n^T$  to  $x_n^0$  through the iterative process defined by

$$x_n^{t-1} = \frac{1}{\sqrt{\alpha_t}} \left( x_n^t - \frac{1 - \alpha_t}{\sqrt{1 - \alpha_t}} \epsilon_\theta(x_n^t | t, z_n) \right) + \sigma_t \epsilon, \quad (13)$$

where  $\sigma_t$  represents the noise level at time step  $t$ , and  $\epsilon$  is sampled from the Gaussian distribution  $\mathcal{N}(\mathbf{0}, \mathbf{I})$ . Ultimately, the decoder in UD-VAE is used to decode all tokens and convert them back into reaction sequences. The overall inference flowchart is shown in Fig. 4.

### More Qualitative Results

In Fig. 5, we provide a qualitative comparison between ReGenNet (Xu et al. 2024) and our proposed MARRS. It can be seen that the human reaction synthesized by our method has more reasonable relative positions and body movements. In particular, our method can generate more natural and plausible hand gestures due to modeling the body and hands separately. We have an additional supplemental video available named **demo.mp4**.

## Offline Setting on NTU120-AS

To demonstrate the adaptability and generalization of our proposed method MARRS, we additionally provide the offline setting results on NTU120-AS in Tab. 7. For the model, we simply adjust the attention mask in the transformer to fit the offline setting. As shown in Tab. 7, MARRS achieves optimal performance on FID and Acc and competitive results on Div and Multimod, highlighting the efficacy of our approach and its adaptability.

### More Experiments on Chi3D-AS Dataset

To evaluate the generalizability of our approach, MARRS, we perform corresponding experiments on another dataset, **Chi3D-AS** (Xu et al. 2024). The open-source model of ReGenNet performs poorly on Chi3D-AS, and its results are different from those reported in the paper. However, the authors did not address this issue. Therefore, we re-train ReGenNet and the corresponding evaluation model using its open source code. We maintain the same experimental setup as described in the paper. The results are shown in Tab. 8. Our proposed MARRS outperforms both MDM (Tevet et al. 2022) and ReGenNet (Xu et al. 2024) across various metrics.

### Model Scalability and Complexity

To evaluate the scalability of MARRS, we present three versions of the model, with sizes of approximately 30M, 60M, and 90M parameters. Details regarding model performance, parameters, training time, and inference time are provided in Tab. 9. We observe that increasing the model size improves overall generation performance, particularly in terms of FID. Furthermore, we compare the parameters, training time, and inference time of MARRS with those of ReGenNet (Xu et al. 2024). The results indicate that MARRS converges more rapidly during training than ReGenNet. In addition, MARRS-Tiny achieves faster inference while maintaining competitive performance.

### User Study

We conduct a user study to evaluate MARRS against ReGenNet (Xu et al. 2024). 20 users were asked to evaluate 32 samples. The results are shown in Fig. 6. Compared to the SOTA method, ReGenNet, about **76%** of users believe that our motions are more *natural*, about **74%** of users believe that our motions are *smoother*, and about **79%** of users believe that our motions are more physically *realistic*.

### Limitation

Due to the lack of high-quality human reaction datasets, we validated the method only on NTU120-AS and Chi3D-AS. In addition, the generated motions exhibit slight foot sliding, which is not yet fully explored in this paper. Owing to the limited accuracy of the current dataset, the generation of certain fine-grained motions (such as finger contacts) is not sufficiently precise. Related researchers in the community are encouraged to explore more challenging aspects of the human reaction synthesis. We hope that MARRS could provide some new insight for the community.



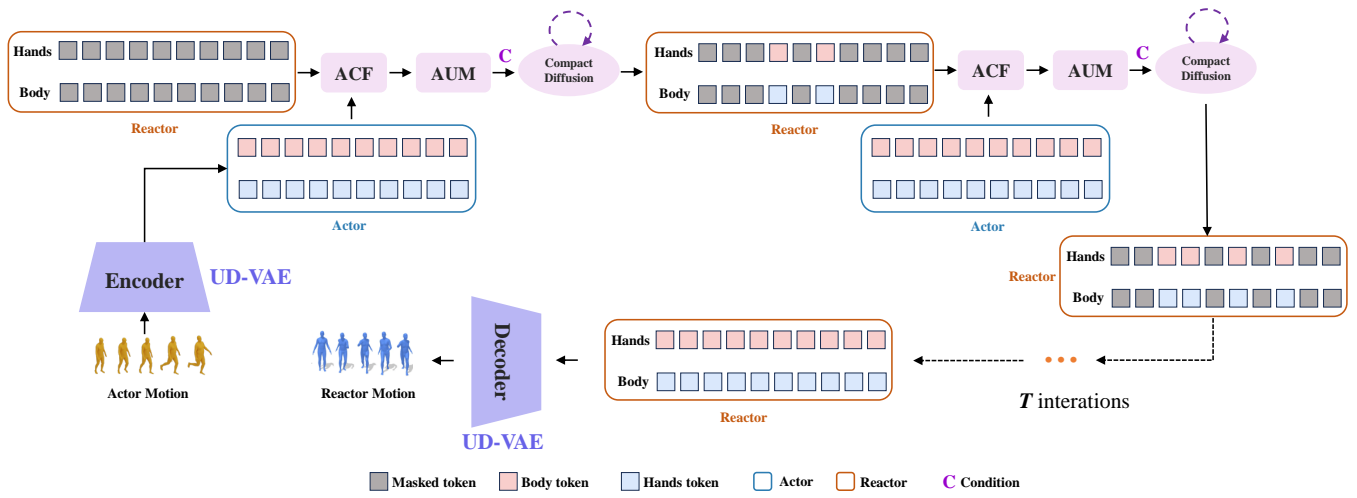


Figure 4: **Visualization of inference process.** The generation of entire tokens is performed in an autoregressive manner. **Compact diffusion** model is very small, consisting of only a 3-layer MLP. Therefore, MARRS can achieve fast inference speed.

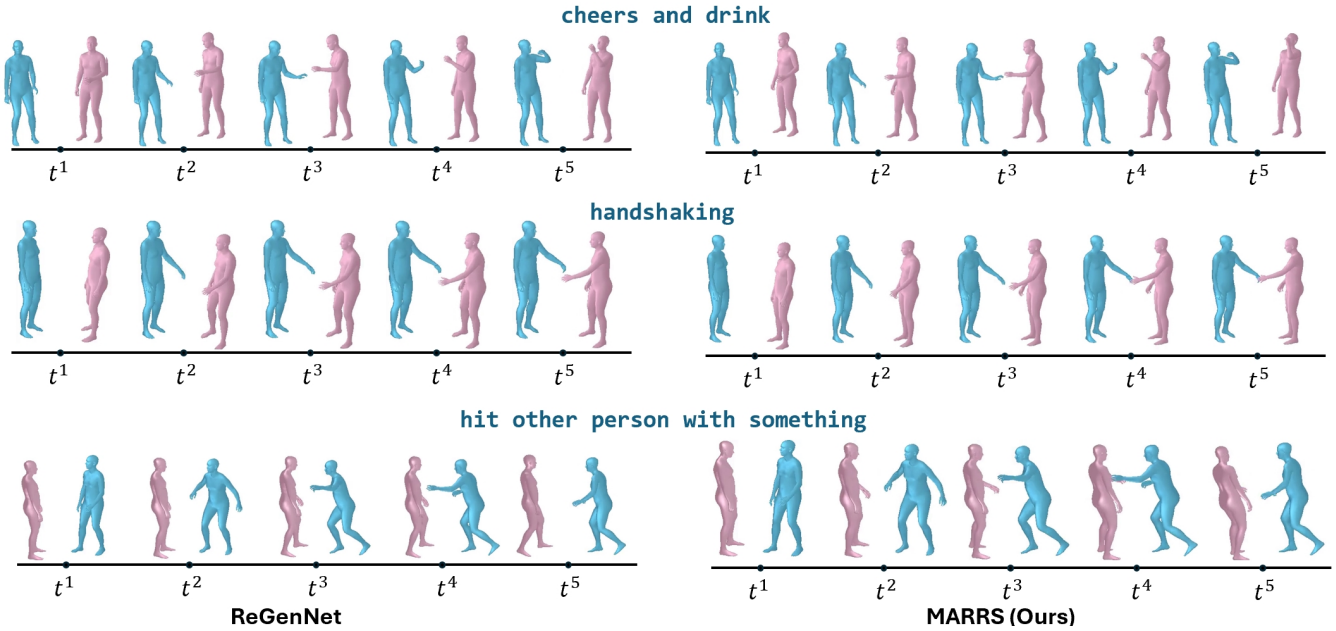


Figure 5: **Qualitative comparison with ReGenNet on human reaction synthesis.** Blue for actors and Red for reactors. The sequences generated by MARRS are more consistent with the action.

Method	FID↓	Acc.↑	Div.→	Multimod.→
Real	0.09±0.00	0.867±0.0002	13.06±0.09	25.03±0.23
cVAE (Kingma, Welling et al. 2013)	74.73±4.86	0.760±0.0002	11.14±0.04	18.40±0.26
AGRoL (Du et al. 2023)	16.55±1.41	0.716±0.0002	13.84±0.10	21.73±0.20
MDM (Tevet et al. 2022)	7.49±0.62	0.775±0.0003	13.67±0.18	24.14±0.29
MDM-GRU (Tevet et al. 2022)	24.25±1.39	0.720±0.0002	<b>13.43±0.09</b>	22.24±0.29
ReGenNet (Xu et al. 2024)	6.19±0.33	0.772±0.0003	14.03±0.09	<b>25.21±0.34</b>
MARRS (Ours)	<b>5.93±0.18</b>	<b>0.783±0.0002</b>	13.96±0.17	<u>25.38±0.50</u>

Table 7: **Results on the offline setting on NTU120-AS (Xu et al. 2024).** ± indicates 95% confidence interval, → means that closer to Real is better. **Bold** indicates the best and underline indicates second best.

Method	Train conditioned				Test conditioned			
	FID↓	Acc.↑	Div.→	Multimod.→	FID↓	Acc.↑	Div.→	Multimod.→
Real	0.19±0.01	1.000±0.000	6.59±0.21	20.96±0.46	0.98±0.22	0.602±0.007	7.71±0.29	12.66±0.35
MDM (Tevet et al. 2022)	12.64±1.85	<b>1.000±0.000</b>	6.88±0.24	19.06±0.29	30.54±3.49	<u>0.443±0.007</u>	6.51±0.59	10.23±0.65
ReGenNet (Xu et al. 2024)	0.28±0.01	<b>1.000±0.000</b>	6.70±0.13	20.75±0.59	<u>21.24±3.42</u>	0.442±0.005	6.96±0.65	<u>10.61±0.90</u>
Ours	<b>0.21±0.01</b>	<b>1.000±0.000</b>	<b>6.69±0.14</b>	<b>20.90±0.57</b>	<b>18.94±2.21</b>	<b>0.480±0.006</b>	<b>7.22±0.53</b>	<b>11.13±0.66</b>

Table 8: **Comparison to state-of-the-arts** on the *online, unconstrained* setting for human action-reaction synthesis on **Chi3D-AS** (Xu et al. 2024). ± indicates 95% confidence interval, → means that closer to Real is better. **Bold** indicates best result and underline indicates second best.

Methods	FID ↓	Acc ↑	Params (M)	Training Time (h)	Inference Time (s)
ReGenNet (Xu et al. 2024)	11.00±0.74	0.749±0.0002	<b>26.8</b>	121	0.058
MARRS-Tiny	10.55±0.62	0.743±0.0003	30.3	<b>10.6</b>	<b>0.039</b>
MARRS-Small	10.12±0.352	0.751±0.0003	56.8	12.7	0.086
MARRS-Base	<b>9.31±0.36</b>	<b>0.753±0.0003</b>	90.2	14.0	0.204

Table 9: **Model scaling results and comparison of computational complexity.** Our proposed MARRS can converge faster in the training process than ReGenNet (Xu et al. 2024) and enlarging the model size can enhance the overall generation performance.

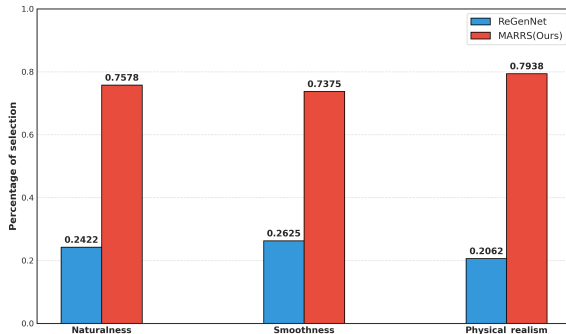


Figure 6: **User study.** We use three subjective indicators, Naturalness, Smoothness, and Physical realism, to compare with the ReGenNet.

## References

- Bethke, E. 2003. *Game development and production*. Wordware Publishing, Inc.
- Chen, X.; Jiang, B.; Liu, W.; Huang, Z.; Fu, B.; Chen, T.; and Yu, G. 2023a. Executing your commands via motion diffusion in latent space. In *Proceedings of the IEEE/CVF Conference on Computer Vision and Pattern Recognition*, 18000–18010.
- Chen, Z.; Li, Z.; Wang, S.; Fu, D.; and Zhao, F. 2023b. Learning from noisy data for semi-supervised 3d object detection. In *Proceedings of the IEEE/CVF International Conference on Computer Vision*, 6929–6939.
- Du, Y.; Kips, R.; Pumarola, A.; Starke, S.; Thabet, A.; and Sanakoyeu, A. 2023. Avatars grow legs: Generating smooth human motion from sparse tracking inputs with diffusion model. In *Proceedings of the IEEE/CVF Conference on Computer Vision and Pattern Recognition*, 481–490.
- Fan, K.; Tang, J.; Cao, W.; Yi, R.; Li, M.; Gong, J.; Zhang, J.; Wang, Y.; Wang, C.; and Ma, L. 2024. Freemotion: A unified framework for number-free text-to-motion synthesis. In *European Conference on Computer Vision*, 93–109. Springer.
- Ghosh, A.; Cheema, N.; Oguz, C.; Theobalt, C.; and Slusallek, P. 2021. Synthesis of compositional animations from textual descriptions. In *Proceedings of the IEEE/CVF international conference on computer vision*, 1396–1406.
- Guo, C.; Mu, Y.; Javed, M. G.; Wang, S.; and Cheng, L. 2024. Momask: Generative masked modeling of 3d human motions. In *Proceedings of the IEEE/CVF Conference on Computer Vision and Pattern Recognition*, 1900–1910.

- Guo, C.; Zou, S.; Zuo, X.; Wang, S.; Ji, W.; Li, X.; and Cheng, L. 2022. Generating diverse and natural 3d human motions from text. In *Proceedings of the IEEE/CVF Conference on Computer Vision and Pattern Recognition*, 5152–5161.
- Kingma, D. P.; Welling, M.; et al. 2013. Auto-encoding variational bayes.
- Komura, T.; Ho, E. S.; and Lau, R. W. 2005. Animating reactive motion using momentum-based inverse kinematics. *Computer Animation and Virtual Worlds*, 16(3-4): 213–223.
- Li, T.; Tian, Y.; Li, H.; Deng, M.; and He, K. 2024. Autoregressive Image Generation without Vector Quantization. *arXiv preprint arXiv:2406.11838*.
- Liang, H.; Zhang, W.; Li, W.; Yu, J.; and Xu, L. 2024. Inter-gen: Diffusion-based multi-human motion generation under complex interactions. *International Journal of Computer Vision*, 1–21.
- Liu, H.; Liu, S.; Zhou, Z.; Xu, M.; Xie, Y.; Han, X.; Pérez, J. C.; Liu, D.; Kahatapitiya, K.; Jia, M.; et al. 2024. Martini: Masked autoregressive diffusion for video generation at scale. *arXiv preprint arXiv:2410.20280*.
- Loshchilov, I.; and Hutter, F. 2017. Decoupled weight decay regularization. *arXiv preprint arXiv:1711.05101*.
- Magenat-Thalmann, N.; Thalmann, D.; Magnenat-Thalmann, N.; and Thalmann, D. 1985. *Computer animation*. Springer.
- Meng, Z.; Xie, Y.; Peng, X.; Han, Z.; and Jiang, H. 2024. Rethinking Diffusion for Text-Driven Human Motion Generation. *arXiv preprint arXiv:2411.16575*.
- Nichol, A. Q.; and Dhariwal, P. 2021. Improved denoising diffusion probabilistic models. In *International conference on machine learning*, 8162–8171. PMLR.
- Parent, R. 2012. *Computer animation: algorithms and techniques*. Newnes.
- Pavlakos, G.; Choutas, V.; Ghorbani, N.; Bolkart, T.; Osman, A. A.; Tzionas, D.; and Black, M. J. 2019. Expressive body capture: 3d hands, face, and body from a single image. In *Proceedings of the IEEE/CVF conference on computer vision and pattern recognition*, 10975–10985.
- Petrovich, M.; Black, M. J.; and Varol, G. 2021. Action-conditioned 3d human motion synthesis with transformer vae. In *Proceedings of the IEEE/CVF international conference on computer vision*, 10985–10995.
- Petrovich, M.; Black, M. J.; and Varol, G. 2022. TEMOS: Generating diverse human motions from textual descriptions. In *European Conference on Computer Vision*, 480–497. Springer.
- Pinyoanuntapong, E.; Wang, P.; Lee, M.; and Chen, C. 2024. Mmm: Generative masked motion model. In *Proceedings of the IEEE/CVF Conference on Computer Vision and Pattern Recognition*, 1546–1555.
- Saridis, G. 1983. Intelligent robotic control. *IEEE Transactions on Automatic Control*, 28(5): 547–557.
- Shafir, Y.; Tevet, G.; Kapon, R.; and Bermano, A. H. 2023. Human motion diffusion as a generative prior. *arXiv preprint arXiv:2303.01418*.
- Shi, Y.; Wang, J.; Jiang, X.; Lin, B.; Dai, B.; and Peng, X. B. 2024. Interactive character control with auto-regressive motion diffusion models. *ACM Transactions on Graphics (TOG)*, 43(4): 1–14.
- Shum, H. P.; Komura, T.; and Yamazaki, S. 2007. Simulating competitive interactions using singly captured motions. In *Proceedings of the 2007 ACM symposium on Virtual reality software and technology*, 65–72.
- Tanaka, M.; and Fujiwara, K. 2023. Role-aware interaction generation from textual description. In *Proceedings of the IEEE/CVF international conference on computer vision*, 15999–16009.
- Tevet, G.; Raab, S.; Gordon, B.; Shafir, Y.; Cohen-Or, D.; and Bermano, A. 2022. Human motion diffusion model. *arXiv preprint arXiv:2209.14916*.
- Urbain, J. 2010. Introduction to game development. *Cell*, 414: 745–5102.
- Wang, S.; Jia, F.; Mao, W.; Liu, Y.; Zhao, Y.; Chen, Z.; Wang, T.; Zhang, C.; Zhang, X.; and Zhao, F. 2024a. Stream Query Denoising for Vectorized HD-Map Construction. In *European Conference on Computer Vision*, 203–220. Springer.
- Wang, S.; Zhao, X.; Xu, H.-M.; Chen, Z.; Yu, D.; Chang, J.; Yang, Z.; and Zhao, F. 2023a. Towards domain generalization for multi-view 3d object detection in bird-eye-view. In *Proceedings of the IEEE/CVF Conference on Computer Vision and Pattern Recognition*, 13333–13342.
- Wang, Y.; Wang, S.; Zhang, J.; Fan, K.; Wu, J.; Jiang, Z.; and Liu, Y. 2024b. Temporal and Interactive Modeling for Efficient Human-Human Motion Generation. *arXiv preprint arXiv:2408.17135*.
- Wang, Z.; Wang, J.; Lin, D.; and Dai, B. 2023b. Intercontrol: Generate human motion interactions by controlling every joint. *arXiv preprint arXiv:2311.15864*.
- Xu, L.; Zhou, Y.; Yan, Y.; Jin, X.; Zhu, W.; Rao, F.; Yang, X.; and Zeng, W. 2024. ReGenNet: Towards Human Action-Reaction Synthesis. In *Proceedings of the IEEE/CVF Conference on Computer Vision and Pattern Recognition*, 1759–1769.
- Yang, J.; Yin, D.; Zhou, Y.; Rao, F.; Zhai, W.; Cao, Y.; and Zha, Z.-J. 2024. MMAR: Towards Lossless Multi-Modal Auto-Regressive Probabilistic Modeling. *arXiv preprint arXiv:2410.10798*.
- Zhang, J.; Zhang, Y.; Cun, X.; Zhang, Y.; Zhao, H.; Lu, H.; Shen, X.; and Shan, Y. 2023a. Generating human motion from textual descriptions with discrete representations. In *Proceedings of the IEEE/CVF conference on computer vision and pattern recognition*, 14730–14740.
- Zhang, M.; Cai, Z.; Pan, L.; Hong, F.; Guo, X.; Yang, L.; and Liu, Z. 2024. Motiondiffuse: Text-driven human motion generation with diffusion model. *IEEE Transactions on Pattern Analysis and Machine Intelligence*.
- Zhang, M.; Guo, X.; Pan, L.; Cai, Z.; Hong, F.; Li, H.; Yang, L.; and Liu, Z. 2023b. Remodiffuse: Retrieval-augmented motion diffusion model. In *Proceedings of the IEEE/CVF International Conference on Computer Vision*, 364–373.

Zheng, C.; and Vedaldi, A. 2023. Online clustered codebook. In *Proceedings of the IEEE/CVF International Conference on Computer Vision*, 22798–22807.

Zou, Q.; Yuan, S.; Du, S.; Wang, Y.; Liu, C.; Xu, Y.; Chen, J.; and Ji, X. 2024. Parco: Part-coordinating text-to-motion synthesis. In *European Conference on Computer Vision*, 126–143. Springer.